Physics 426 - Instability Notes

Jody Klymak

March 20, 2020

1 Introduction

The study of turbulence is necessarily hampered by the fact that turbulence is inherently strongly non-linear. In the previous notes we saw that variance grows at the most unstable wavenumber quickly, but it also cascades to higher and lower wavenumbers. This is due to those modes growing, but also due to the fast-growing modes interacting with one another randomly and eventually tearing each other apart into turbulence. This is seen in detail in a numerical simulation (figure 1 on the following page) where only two vortices are created, but they still interact with one another and create homogeneous turbulence.

If the Reynolds number of the flow is great enough, the flow develops what we call "homogeneous" turbulence, where the turbulent fluctuations stop carrying a memory of the instability that formed them and they have universal statistical properties.

2 Turbulent scales and spectra

These universal statistical properties are often expressed as power spectra. So while we do not know what the velocity or value of any particular tracer is at any time or place, we can characterize its variance as a function of frequency and wavenumbers. An example of this was shown in the previous write up. Another example is shown in figure 2 on page 3 for the simulation in figure 1 on the following page and compared to observations.

This was of thinking about turbulence leads to a few very powerful, but ultimately empirical results. These results largely follow from dimensional analysis which is surprisingly effective in this context.

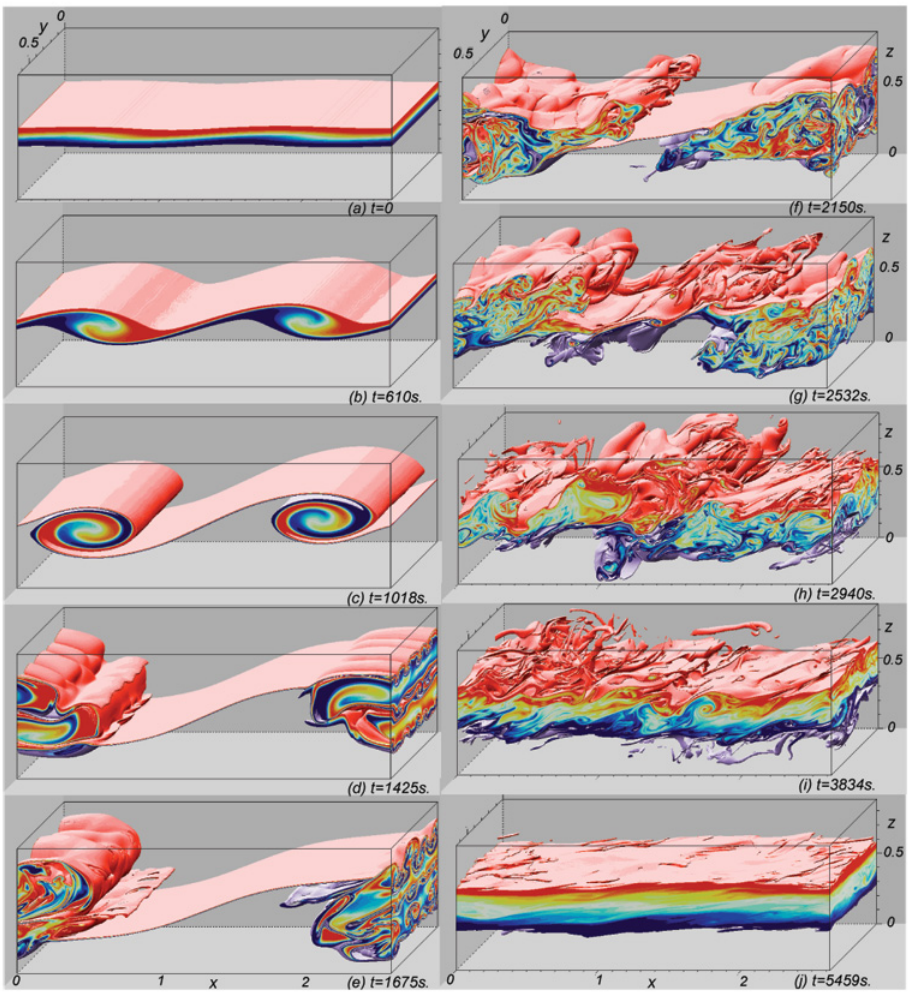

Figure 1: Numerical simulation [Smyth et al., 2005] of a shear isntability transitioning to turbulence.

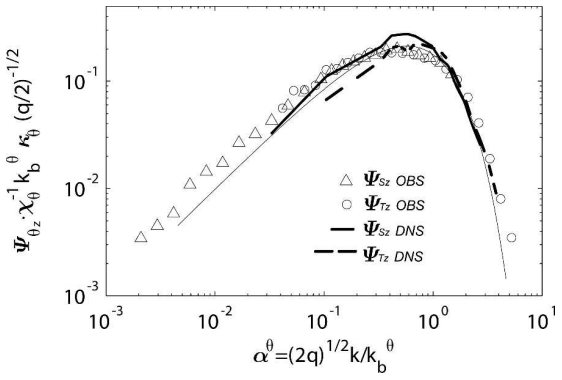

Figure 2: Power spectra of tracer variance from [Smyth et al., 2005] compared to oceanic observations of tracer spectra. The wavenumber k has been scaled to match a universal form

2.1 Kolmogorov wavenumber and Inertial subrange

First, it is important to determine the variables that are important to the turbulence. In steady state, the rate that energy is put into the turbulence is equal to the rate that it is removed, by viscous dissipation, which we usually denote ϵ [$\mathrm{m^2\,s^{-3}}$]. The other variable that sets the scale at which viscosity overcomes the turbulence is the strength of the viscosity ν [$\mathrm{m^2\,s^{-1}}$]. These two variables combined set the scale at which turbulent fluctuations die off, which we represent by a wavenumber $k_\nu = \epsilon^{1/4}\nu^{-3/4}$. This scale is small for most flows and actually gets smaller as the strength of the turbulence (ϵ) increase. In a turbulent channel in the waters near here, $\epsilon \approx 10^{-4}$ $\mathrm{m^2\ s^{-3}}$ we get a value of $k_s \approx 3000$ rad/m or a length scale of 1 mm. This wavenumber, k_s, is called the Kolmogorov wavenumber. We can similarly use scaling analysis to say that the shortest time scale of motion is $t_\nu \approx (\nu/\epsilon)^{1/2}$.

This scaling works very well for predicting the scale at which turbulence decays. Measurements in Knight Inlet BC made by Ann Gargett (who is an emeritus professor here) show that as the wavenumber approaches k_s the power spectrum of the velocity variance drops off rapidly (figure 3 on the next page).

It is also relatively clear that the spectra have a universal slope at lower wavenumbers. This region of wavenumber space between the viscous subrange and the large scales at which energy in input is called the "inertial

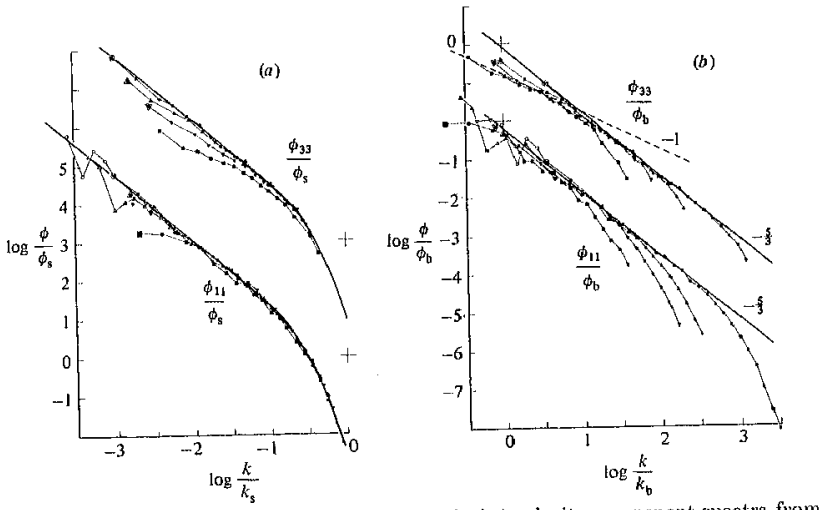

Figure 3: Power spectra of a) velocity and b) tracer variance collected from a submersible in Knight Inlet [Gargett et al., 1984]. In a) the horizontal wavenumber is scaled by the Kolmogorov scale k_s. In b) it is normalized by the Batchelor wavenumber.

subrange". In this subrange, the spectrum only depends on the strength of the turbulence, ϵ and the wavenumber k. A velocity spectrum ϕ in wavenumber space has units of $\mathrm{m^2 s^{-2}/cpm}$ or $\mathrm{m^3\,s^{-2}}$, so dimensional analysis says that $\phi \sim \epsilon^{2/3} k^{-5/3}$, and indeed this is the slope of the spectra shown in figure 3a.

2.2 Tracer subranges

For a passive tracer, variance is destroyed at a rate χ $[\mathrm{K^2 s^{-1}}]$, by diffusion κ instead of viscosity. For instance for heat, variance is smoothed out by thermal diffusion. In this case the smallest scale of variance depends on three variables, ϵ, ν and κ. Since κ and ν have the same units we cannot appeal just to dimensional analysis to determine the power laws, but instead consider that the Batchelor scale is the scale at which the time to dissipate the energy at that scale is equal to the time it takes to diffuse the variance away, yielding $k_b = \epsilon^{1/4} \nu^{-1/4} \kappa^{-2/4}$.

Hence for a tracer, we have a complicated situation where energy is put in at large scales (figure 4 on the next page), there is an "inertial subrange" where both momentum and the tracer are stirred in tandem ($k < k_*$). In

this range $\phi_T \sim k^{-5/3}$, or in figure 4, $\phi_{dT/dz} \sim k^{1/3}$. At some point viscosity becomes important, and the power law changes to depend on k, ϵ, χ, *and* ν. These do not uniquely give the power law in the next subrange, called the "viscous-convective" subrange, but it turns out that $\phi_T \sim k^{-1}$ (or $\phi_{dT/dz} \sim k^1$) as in figure 4). The third subrange is the "diffusive" subrange where diffusivity finally becomes important at the highest wavenumbers.

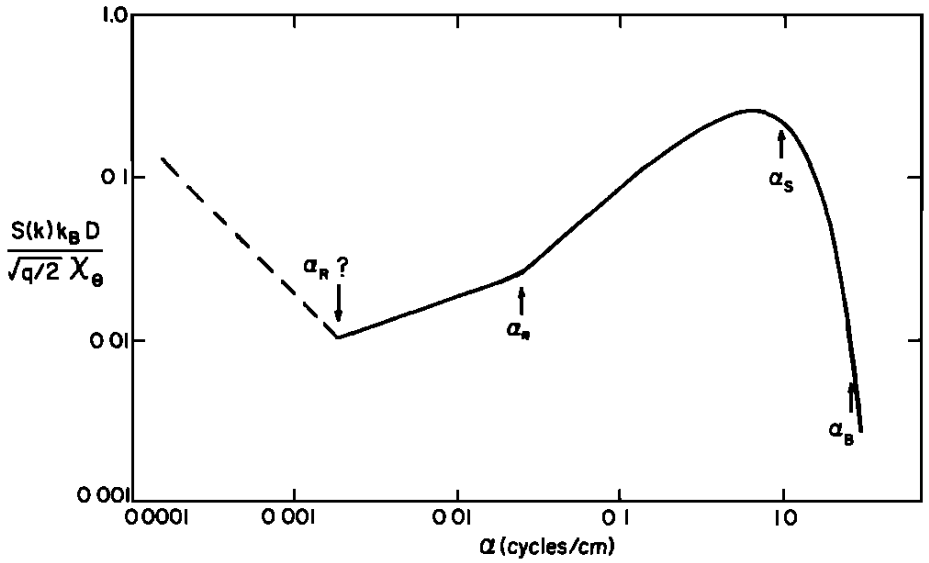

Figure 4: Schematic temperature gradient spectrum [Dillon and Caldwell, 1980]. α_* is the scale to which momentum and tracer are stirred without the effect of viscosity. α_s is the Kolmogorov wavenumber, and α_B is the Batchelor wavenumber.

The universality of these spectral shapes is quite impressive for high-Reynolds number flows, such as those found in the ocean figure 5 on the following page, though it is notoriously hard to observe the viscous subrange because it is so small. The measurements made in figure 5 on the next page are possibly using a small-scale thermocouple, but this instrumentation is not very long lasting in seawater.

As a note on the universality of the spectra - this has mostly only been shown in geophysical flows where there is a large scale separation between the Kolmogorov scale and/or Batchelor scale and the scale at which shear

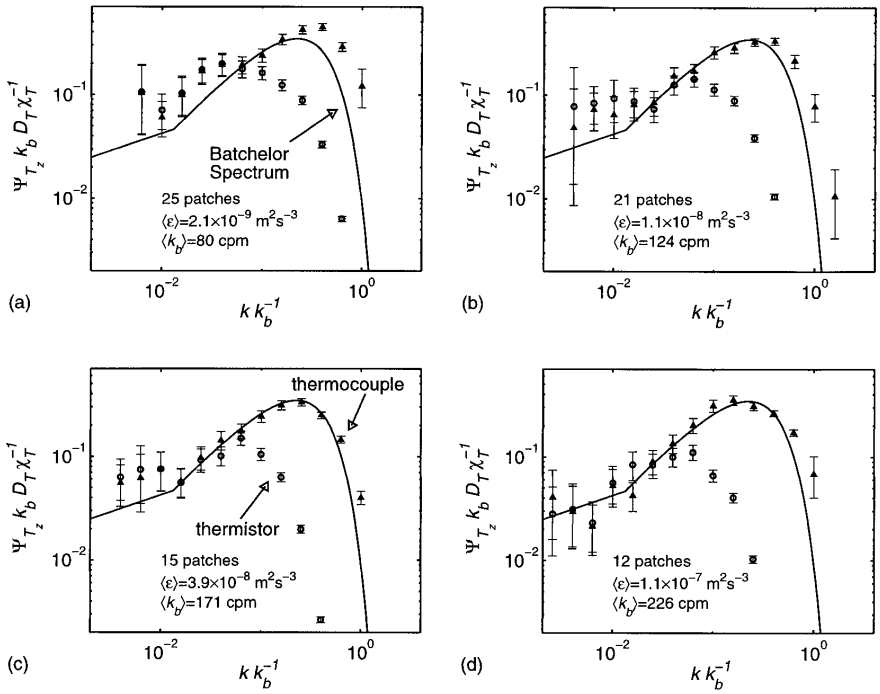

Figure 5: Spectra of temperature gradient measured in the ocean using a small-scale thermistor, and a smaller thermo-couple [Nash et al., 1999]. Note the Batchelor scale is order 4 mm to 1 cm in these measurements, and it is very hard to make measurements to such small scales.

develops. For a small pipe, a few centimeters across, the Kolmogorov scale may be less than an order of magnitude smaller than the pipe, and that may not be enough "wavenumber space" for an inertial subrange to develop. Hence the first observations of these universal spectra were made in very energetic turbulence in the ocean - the first such observation was made by Grant et al. [1962] based out of DREP in Esquimalt by taking velocity measurements in Seymour Narrows between Vancouver Island and Quadra Island.

2.3 Measuring turbulence

Measuring turbulence is notoriously difficult. In the laboratory, it requires small-scale velocity measurements. Approaches include

- High-frequency acoustic measurements that depend on the time-of-flight of sound pulses or the Doppler effect on particles in the water.
- Sheets of lasers on suspended particles in the fluid and video cameras that track the motion of the particles in the sheets.
- Temperature probes to measure small-scale fluctuations in temperature.

Geophysical measurements are hard in that they often have trouble contextualizing the flow that the turbulence is found in. However, they have the advantage that the turbulence is very strong, and hence the measurements can be a bit cruder. In the ocean, we either tow or profile vehicles (figure 6 on the following page) equipped with shear probes and high-speed thermistors (figure 7 on the next page). An example from my thesis exhibits some of the challenges with these methods (figure 8 on page 9). These are measurements from Knight Inlet, with strong stratified tidal flow over an underwater sill. Collected with a vertical profiling instrument, the data collection is sparse compared to the size of the flow, and multiple repeat passes over the sill necessary to characterize the flow. However, the flow is constantly changing over the 12.4-h tidal cycle, so even these snapshots are fragmentary.

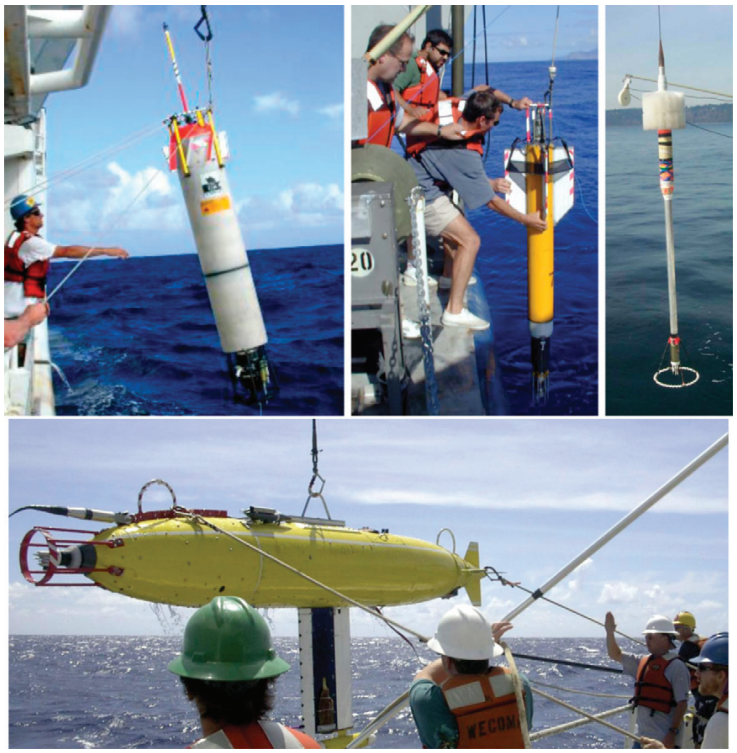

Figure 6: Oceanic vehicles for measuring ocean turbulence [Klymak and Nash, 2009]. The upper three are vertical profilers that fall freely from a ship. The bottom is a towed instrument, similar to that used by Grant et al. [1962], Gargett et al. [1984].

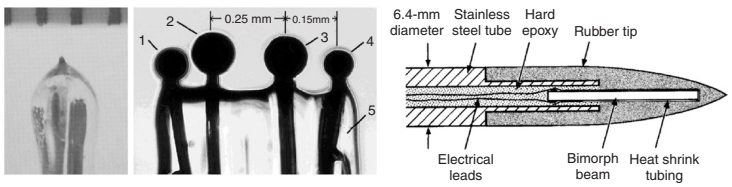

Figure 7: Probes for measuring ocean turbulence [Klymak and Nash, 2009]. Left, a fine-scale thermistor, a (fragile) microconductivity probe (with two anodes and two electrodes), and a piezo-electric shear probe.

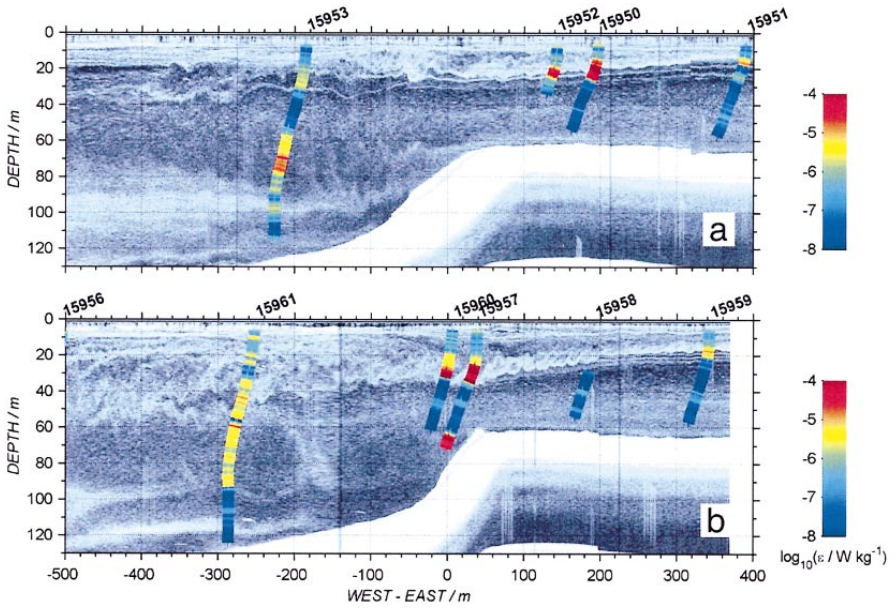

Figure 8: Turbulence measured from a turbulence profiler deployed in Knight Inlet [Klymak and Gregg, 2004]. Flow is visualized using high-frequency acoustics scattering off both biology (zooplankton) and sharp gradients in salt caused by turbulence (and of course the seafloor). The colored tracks are turbulence dissipation rates measured by the profiler. The flow is from right to left, and is blocked by the sill creating a hydraulic flow similar to the ones studied in class.

3 Turbulent fluxes

Turbulence leads to much faster diffusion of momentum and tracers. Ultimately, mixing of momentum and tracers must occur at the molecular level on scales that are quite small. Turbulence stirs the fluid and greatly increases the area over which molecular diffusion acts, as well as acting to sharpen gradients which also increases turbulence fluxes (figure 9).

The approach we use to quantify this extra mixing is at its heart empirical. However, some important quantities in this empirical exercise can be derived if we divide the flow into "mean" and "fluctuating" components in a procedure known as "Reynolds Averaging".

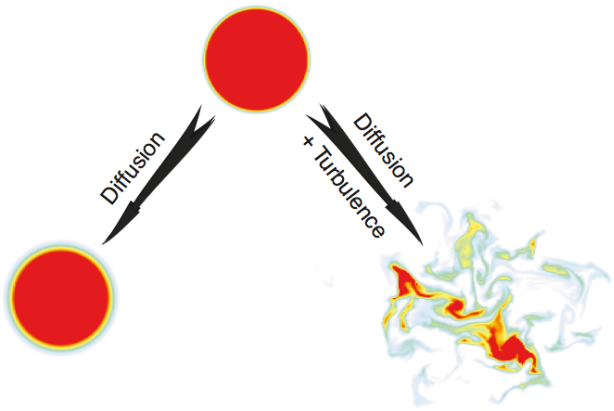

Figure 9: Schematic of the importance of turbulence stirring to molecular diffusion.

Here we write the equations of motion and decompose into a mean component and a fluctuating component (denoted with primes). For reference, the full equations of motion, including a buoyancy term due to the temperature of the water are:

$$\begin{aligned}
\frac{\partial \tilde{\mathbf{u}}}{\partial t} + \tilde{\mathbf{u}} \cdot \nabla \tilde{\mathbf{u}} &= -\frac{1}{\rho}\nabla \tilde{p} - g\left[1 - \alpha(\tilde{T} - T_0)\right]\mathbf{k} + \nu \nabla^2 \tilde{\mathbf{u}} \\
\nabla \cdot \tilde{\mathbf{u}} &= 0 \\
\frac{\partial \tilde{T}}{\partial t} + \tilde{\mathbf{u}} \cdot \nabla \tilde{T} &= \kappa \nabla^2 \tilde{T}
\end{aligned}$$

where we have included a buoyancy term in the z momentum equation and α is a "thermal expansion" co-efficient that is linear around T_0.

The Reynolds decomposition is to then say

$$\begin{aligned}\tilde{\mathbf{u}} &= \mathbf{U} + \mathbf{u}' \\ \tilde{p} &= P + p' \\ \tilde{T} &= T + T'\end{aligned}$$

where over some spatial or temporal interval the turbulent quantities are zero: $\overline{\mathbf{u}'} = \overline{p'} = \overline{T'} = 0$.

These are then substituted into the equations of motion:

$$\begin{aligned}\frac{\partial(\mathbf{u}+\mathbf{U})}{\partial t} + (\mathbf{u}+\mathbf{U})\cdot\nabla(\mathbf{u}+\mathbf{U}) &= -\frac{1}{\rho}\nabla(P+p') - g\left[1-\alpha(T+T'-T_0)\right]\mathbf{k} + \nu\nabla^2(\mathbf{u}+\mathbf{U}) \\ \nabla\cdot(\mathbf{u}+\mathbf{U}) &= 0 \\ \frac{\partial(T+T')}{\partial t} + (\mathbf{u}+\mathbf{U})\cdot\nabla(T+T') &= \kappa\nabla^2(T+T')\end{aligned}$$

And then we take the same average that defined the Reynolds decomposition. i.e. for the continuity equation:

$$\overline{\nabla\cdot(\mathbf{u}+\mathbf{U})} = \nabla\cdot\mathbf{U} + \overline{\nabla\cdot\mathbf{u}} = 0 \tag{1}$$

But the second term averages to zero because $\overline{\nabla\cdot\mathbf{u}} = \nabla\cdot\overline{\mathbf{u}} = 0$, so this means that $\nabla\cdot\mathbf{U} = 0$. Subtracting from the full continuity equation this means that $\nabla\cdot\mathbf{u} = 0$ as well.

The same procedure on the momentum equation yields an equation for the slowly evolving flow of:

$$\frac{\partial\mathbf{U}}{\partial t} + \mathbf{U}\cdot\nabla\mathbf{U} + \overline{\mathbf{u}\cdot\nabla\mathbf{u}} = -\frac{1}{\rho}\nabla P - g\left[1-\alpha\left(T-T_0\right)\right]\mathbf{k} + \nu\nabla^2\mathbf{U} \tag{2}$$

where the only term that remains from the turbulent quantity is the quadratic term in $\mathbf{u}$.

The terms represented by $\overline{\mathbf{u}\cdot\nabla\mathbf{u}}$ are the turbulent stresses, as opposed to the viscous stresses that are encapsulated by the last term. This is the only place in this class where Einstein notation would be very useful, but lets just write out the x-momentum terms of this equation

$$\begin{aligned}\overline{\mathbf{u}\cdot\nabla\mathbf{u}}\cdot\mathbf{i} &= \overline{u\frac{\partial}{\partial x}u} + \overline{v\frac{\partial}{\partial y}u} + \overline{w\frac{\partial}{\partial z}u} \\ &= \frac{\partial}{\partial x}\overline{u^2} + \frac{\partial}{\partial y}\overline{uv} + \frac{\partial}{\partial z}\overline{uw}\end{aligned}$$

and then we note the analogue to the viscous terms in the x-momentum equation:

$$\nu\nabla^2\mathbf{U}\cdot\mathrm{i} \;=\; \frac{\partial}{\partial x}\left(\nu\frac{\partial U}{\partial x}\right)+\frac{\partial}{\partial y}\left(\nu\frac{\partial U}{\partial y}\right)+\frac{\partial}{\partial z}\left(\nu\frac{\partial U}{\partial z}\right)$$

where recall that we said the viscous stress transporting x-momentum in the z-direction was $\tau_{xz} = -\nu\frac{\partial U}{\partial z}$. So in direct analogy, we say that $-\overline{uw}$ is the turbulent stress that carries x-momentum in the z-direction. Similarly $-\overline{uv}$ is turbulent stress carrying x-momentum in the z-direction and $-\overline{u^2}$ is turbulent stress carrying x-momentum in the x-direction.

To better understand this transfer of momentum, consider a flow in the x-direction that is sheared in the vertical (figure 10). If there is a turbulent $w < 0$ in the flow, it tends to bring faster water down with it, meaning on average $u > 0$, and hence $-\overline{uw} > 0$ and positive x-momentum is transfered down. Exactly the same direction of momentum transfer happens if $w > 0$ and transporting slower fluid up in the water column, and hence the average of $-\overline{uw}$ is a "stress" on the flow seeking to homogenize the momentum. This is the same sense that the momentum is homogenized molecularly by τ_{xz}.

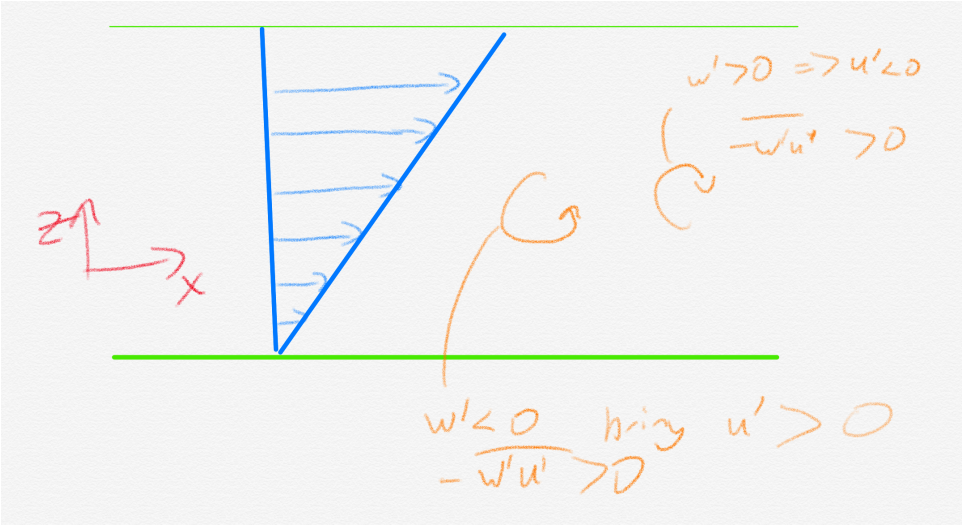

Figure 10: Sketch of sheared flow and the effect of positive and negative fluctuations in w' on the flow.

Given the analogy with molecular viscous stress, its quite natural to seek a parameterization of the turbulent stresses in terms of the large scale flow,

and indeed this is what is done in numerical simulations that cannot hope to resolve the full spectrum of turbulence. In the most general case we say

$$\overline{\mathbf{u} \cdot \nabla \mathbf{u}} = \kappa_T \nabla^2 \mathbf{U} \tag{3}$$

which is equivalent to saying that the turbulent stress is proportional to the *mean* shear. e.g. for the x-momentum equation:

$$\overline{\mathbf{u} \cdot \nabla \mathbf{u}} \cdot \mathbf{i} = \kappa_T \nabla^2 U \tag{4}$$

In general κ_T is *much* larger than ν and the turbulent mixing dominates the molecular. The challenge, of course, is knowing what κ_T should be. This is an empirical and field-dependent endeavour, and is still a topic of heavy research.

4 Notes on numerically simulating turbulent flows

Turbulent flows are very hard to simulate numerically. In 2020, a super-large gigantic super computer cluster consists of 64k cores. A good rule of thumb is no more than domain sizes that as 64^3 in size. If we divide the 64k cores evenly among all three directions, we get a domain size of $256k$ cells in each direction. If we are to resolve the Kolmogorov scale for moderately strong turbulence of $\epsilon \sim 10^{-6}$ m^{2}s^{-3}, then $\eta = 1$mm and our numerical simulation will extend 256 m in each direction. This would be a truly fabulous simulation but extremely expensive as we would also have to resolve the CFL criteria of the flow. In the ocean this is on the order of 1 m/s, so our 1 mm grid cells would require timesteps of less than 0.001 s. The problem worsens when the dissipation rate increases.

Such expensive *direct numerical simulations* (DNS) are not generally carried out, and whenever DNS is applied usually much smaller domains are considered (i.e. figure 1 on page 2). A less intensive method to approximate turbulence is to suppose that the model resolves the big billows in the instability, i.e. the roll-ups in figure 1 on page 2, and then applies an enhanced viscosity where it resolves strong shear. The strength of this enhanced viscosity does not matter too much because it generally just acts to destroy whatever is caught in the roll-up. This approach is called *large eddy simulation* (LES) and is naturally less precise than DNS, but only needs resolution on the scale of the breaking eddies (say 10-s of cm) versus the Kolmogorov scale (mm).

Finally, there are even cruder parameterizations that apply when the simulation cannot resolve the turbulent roll-ups. For instance a global ocean

simulation will often be run at scales of 10-s of kilometers (or 100s) and will have no hope of simulating shear instabilities, even relatively large ones like we would find in large-scale lateral instabilities. In these cases, turbulence is usually estimated from large-scale shear $\partial U/\partial z$ and the change of stratification $\partial \rho/\partial z$. If the ratio of these becomes too high, the flow is assumed to become turbulent and mixing is applied until the ratio drops again. In general this works fine to keep the model running, but it will drift from observed conditions over longer time scales, and hence the model usually needs to be nudged back to reality via assimilation of observations.

References

T. M. Dillon and D. R. Caldwell. The Batchelor spectrum and dissipation in the upper ocean. *J. Geophys. Res.*, 85(C4):1910–1916, 1980.

A. E. Gargett, T. R. Osborn, and P. W. Nasmyth. Local isotropy and the decay of turbulence in a stratified fluid. *J. Fluid Mech.*, 144:231–280, 1984. Shows that buoyancy suppresses turbulence in vertical direction. Horizontal spectrum extends further than vertical.

H. L. Grant, R. W. Stewart, and A. Moilliet. Turbulence spectra from a tidal channel. *J. Fluid Mech.*, 12:241–268, 1962.

J. M. Klymak and M. C. Gregg. Tidally generated turbulence over the Knight Inlet sill. *J. Phys. Oceanogr.*, 34(5):1135–1151, 2004.

J. M. Klymak and J. D. Nash. Estimates of mixing. In J. H. Steele, K. K. Turekian, and S. A. Thorpe, editors, *Encyclopedia of Ocean Sciences*, chapter Estimates of Mixing, pages 3696–3706. Academic Press, 2009. doi: DOI: 10.1016/B978-012374473-9.00615-9. URL `http://www.sciencedirect.com/science/article/B99B0-4V2BCCJ-DC/2/2ca8446f1fd15696e37`

J. D. Nash, D. R. Caldwell, M. J. Zelman, and J. N. Moum. A thermocouple for high-speed temperature measurements in the ocean. *J. Atmos. Ocean. Tech.*, 16:1474–1483, 1999.

W. D. Smyth, J. Nash, and J. Moum. Differential diffusion in breaking Kelvin-Helmholtz billows. *J. Phys. Oceanogr.*, 35:2753–2766, 2005. doi: 10.1175/JPO2739.1.